Asymptotic Spectral Efficiency of Multicell MIMO Systems with Frequency-Flat Fading*

Huaiyu Dai*, *Member, IEEE* and H. Vincent Poor, *Fellow, IEEE*+

Abstract

In this paper, the spectral efficiency of multiple-input multiple-output (MIMO) systems operating in multicell frequency-flat fading environments is studied, for situations in which co-channel interference is the dominant channel impairment instead of ambient noise. The following detectors are analyzed: the joint optimum detector, a group linear minimum-mean-square-error (MMSE) detector and its generalized version, a group MMSE successive interference cancellation detector, and an adaptive multiuser detector, with the focus on their large-system asymptotic (non-random) expressions. Analytical and numerical results based on these asymptotic multicell MIMO spectral efficiencies are explored to gain insights into the behavior of interference-limited multicell MIMO systems.

Index Terms: Channel capacity, co-channel interference, cellular communications, large-system asymptotic analysis, MIMO systems, multiuser detection, spectral efficiency

EDICS: 2-INFO

---

* This research was supported in part by the National Science Foundation under Grant CCR 99-80590, and in part by the New Jersey Center for Wireless Telecommunications.
+ H. Dai was with the Department of Electrical Engineering, Princeton University. He is now with the Department of Electrical and Computer Engineering, NC State University, Raleigh, NC 27695-7511. Phone: (919) 513-0299; Fax: (919) 515-2285; Email: Huaiyu_Dai@ncsu.edu. H. V. Poor is with the Department of Electrical Engineering, Princeton University, Princeton, NJ 08544. Email: poor@princeton.edu.

I. Introduction

Recent information theoretic results have suggested the remarkable capacity potential of wireless communication systems with antenna arrays at both the transmitter and receiver. These multiple-input multiple-output (MIMO) systems have been shown, in principle, to yield unprecedented capacity, which grows at least linearly with the number of antennas [13], [27], when operating in an isolated cell with white Gaussian background noise only. However, achieving this capacity in real cellular environments can be problematic. In this situation, the co-channel interference from surrounding cells is typically the dominant channel impairment and greatly diminishes MIMO system capacity.

A recent study by Catreux et al. [6] indicated the ineffectiveness of a MIMO system in such an interference-limited environment. This seems to be related to an insufficient number of degrees of freedom of MIMO systems at the receiver side to suppress the co-channel interference. On the other hand, this investigation assumed a certain system structure (uncoded V-BLAST) taken from the noise-limited case, and did not try to optimize the system for interference-limited environments. Motivated by this study, in previous work the authors and Molisch showed that the performance of MIMO systems can be improved significantly in a multicell structure, through application of advanced signal processing techniques [8]. In particular, we employed a turbo space-time multiuser receiver structure for intracell communication, which essentially approaches the Shannon limit (within 1-2 dB) for an isolated cell. Furthermore, we used another level of multiuser detection to combat the intercell interference. Among various multiuser detection (MUD) techniques examined, *group linear MMSE*[1] *MUD* and *group MMSE successive interference cancellation* were shown to be feasible and effective. Based on these two multiuser detection schemes, each of which may outperform the other for different settings, an *adaptive multiuser detection* scheme was also proposed. Simulation results indicated significant performance improvement of our approach over the well-known V-BLAST techniques with coding. Nevertheless, it was also found that there is a significant performance gap between the obtained MUD capacity and the interference-free capacity upper bound in environments with strong interference.

In this paper, we study the underlying rationale of the advantages and limitations of the receiver structures proposed in [8]. In particular, spectral efficiencies [32], i.e., the total number of bits per second per hertz (bits/s/Hz) that can be reliably supported by a system *with these receivers* are derived and compared with those with other receivers of interest. Assuming that channel state information (CSI) is not known to the transmitter, we assign the total transmitted power equally to all

[1] Minimum-mean-square-error

substreams of a MIMO system[2] [13], [27]. It is also well verified in the literature (see. e.g., [32]) that unless E_b / N_0 is very low, the gain in spectral efficiency achievable by optimum power allocation is small enough not to warrant the required increase in complexity, especially when the system size (number of users, antennas, subcarriers, etc.) becomes large. Please note that the spectral efficiency studied in this paper is in general not the real channel capacity, as optimal power allocation is not attempted and some suboptimal receiver front-ends are used. Rather, the purpose is to study and compare the performance of several multiuser MIMO receivers of interest under a common realistic setting. We always assume optimal detection[3] for intracell communication, so the receivers are differentiated by the multiuser detection methods used to combat the intercell interference, i.e., *the joint optimum detector, a group linear MMSE detector, a group MMSE successive interference cancellation detector,* and *an adaptive multiuser detector*. We develop asymptotic results as the network dimensions grow, based on the application of analytical results on the eigenvalue distributions of large random matrices [25], [26]. That is, we consider the limiting region where both the number of transmit antennas K and receive antennas N go to infinity, while their ratio remains constant. Besides its analytical convenience, the study of large system performance also has practical advantages: what is revealed in the asymptotic limit is fundamental in nature, which may be concealed in the finite case by random fluctuations and other transient properties of the matrix entries; moreover, the convergence to the asymptotic limit is typically rather fast as the system size grows. The asymptotic analysis has been carried out both for MIMO systems [2], [27] and CDMA systems with random signatures [23], [32] before, and is readily applied to this study.

The main results of this paper can be summarized as follows.

1. Theoretical capacity bounds are derived for several multicell MIMO receivers, which agree well with and provide further insight into related signal processing results in [8].

2. Simple relations are found among these capacity formulas. In particular, the spectral efficiencies of group linear MMSE detectors, group MMSE successive interference cancellation detectors, and adaptive multiuser detectors can all be expressed in forms related to the spectral efficiency of the joint optimum detector (see (30), (33), (42) and (49)). This makes their asymptotic large-system expressions easy to obtain through that of the joint optimum detector.

[2] That is, the inputs are not only totally power-constrained, but also individually power-constrained.

[3] As a practical matter, optimal single-cell detection can be approximated by turbo space-time multiuser detection (see, e.g., [8]).

3. Both exact and approximate formulas are given for the asymptotic (non-random) spectral efficiency of the joint optimum detector. The approximate formula agrees very well with the exact one for a wide range of settings, while avoiding complex operations such as fixed-point solutions of high-order polynomial equations and computation of definite integrals. Expressed only with standard functions, the approximate formula proves very useful for theoretical analysis (see Appendix I and II).

4. Conditions for non-interference-limited behavior of the group linear MMSE detector are found and verified. Based on these conditions, tradeoffs among system load, energy, receiver complexity and achievable capacity for multicell MIMO system design are discussed.

This paper is organized as follows. Section II presents the system model and empirical eigenvalue distributions of some large random matrices that will be useful in the sequel. In Section III, formulas are derived for the asymptotic spectral efficiencies of multicell MIMO systems with several optimum and sub-optimum detectors. In Section IV, some analytical and numerical results based on these asymptotic multicell MIMO spectral efficiencies are given. Finally, Section V contains some concluding remarks.

II. System Model

A. MIMO System Model

For single-cell MIMO systems, we adopt the same mathematical model as in [13] and [27], given by

$$\mathbf{y} = \mathbf{H}\mathbf{x} + \mathbf{n}, \tag{1}$$

where $\mathbf{y}$ is the received vector corresponding to the outputs of N collocated receive antennas, $\mathbf{x}$ contains the independent substreams transmitted by K collocated transmit antennas, $\mathbf{H}$ is an $N \times K$ channel matrix that captures the channel characteristics between transmit and receive antenna arrays, and $\mathbf{n}$ is the background noise. Throughout this paper, we assume $N \geq K$, and define $\beta = K/N$ to be the system load. The entries of $\mathbf{H}$ are independent and identically distributed (i.i.d.) normalized complex Gaussian random variables, modeling a Rayleigh flat fading channel with adequate physical separation between transmit and receive antennas. The noise is assumed to be circularly symmetric complex Gaussian with covariance matrix $\mathbf{\Phi}_{\mathbf{n}} = \sigma^2\mathbf{I}$, where $\mathbf{I}$ denotes an identity matrix. We assume that the total transmitted power is constrained to be no larger than P, and is equally assigned to the independent substreams due to the lack of channel state information at the transmitter, i.e., $E\{\mathbf{x}\mathbf{x}^H\} = (P/K)\mathbf{I}$. The signal-to-noise ratio (SNR) is given by $\rho = P/\sigma^2$. The channel state information is always assumed to be known at the receiver.

B. Multicell Communication Model

In the literature, multicell systems are often addressed with the attractive infinite linear array model (i.e., Wyner's model [33]):

$$\mathbf{y} = \mathbf{H}\mathbf{x} + \alpha\mathbf{H}^{-}\mathbf{x}^{-} + \alpha\mathbf{H}^{+}\mathbf{x}^{+} + \mathbf{n}\ , \tag{2}$$

where only the adjacent-cell interference is taken into account, characterized by a single attenuation factor $0 \le \alpha \le 1$. In this paper, we adopt a more general multicell model given as follows [24], [8]:

$$\mathbf{y} = \mathbf{H}\mathbf{x} + \sum_{i=1}^{L} \alpha_i \mathbf{H}_{ifi}\mathbf{x}_{ifi} + \mathbf{n}\ , \tag{3}$$

where we assume without loss of generality that $0 \le \alpha_L \le \cdots \le \alpha_1 \le 1$ with L denoting the number of effective interfering cells. In the sequel, we sometimes assign the desired cell index 0 with the understanding that $\alpha_0 = 1$ for convenience. The signals, channels and background noise for all the cells are assumed to be mutually independent and follow the same assumptions given in Subsection II.A. The signal-to-noise ratio is given by $\rho = P/\sigma^2$ as before, and the signal-to-interference ratio (SIR) is given by $\mu = 1\Big/\sum_i \alpha_i^2$. We focus mainly on the case in which all the cells are identical with one active MIMO user in each[4], and all the MIMO users operate at the same rate, which is further distributed among K substreams equally.

C. Empirical Distribution of a Random Eigenvalue

Suppose $\mathbf{A}$ is a $p \times p$ matrix with all real eigenvalues. The empirical distribution function of the eigenvalues of $\mathbf{A}$ is defined as $F^{\mathbf{A}}(x) = \frac{1}{p}\#(\lambda_{\mathbf{A}} \le x)$ with "#" denoting the cardinality, which refers to the relative proportion of eigenvalues of $\mathbf{A}$ that lie below x. Equivalently, $F^{\mathbf{A}}$ can be viewed as the cumulative distribution function of a uniformly randomly selected eigenvalue of $\mathbf{A}$. The following theorem is needed to calculate the asymptotic spectral efficiency of MIMO systems. This theorem requires the definition of the Stieltjes transform for any distribution function G, given as

$$m_G(z) = \int \frac{1}{\lambda - z} dG(\lambda) \tag{4}$$

for $z \in C^{+} \triangleq \{z \in C : \operatorname{Im} z > 0\}$.

---

[4] This model includes systems using TDMA, FDMA or orthogonal CDMA.

Theorem II.1 [25]: Suppose $\mathbf{X}$ is an $N \times n$ matrix containing i.i.d. complex entries with unit variance, and $\mathbf{T}$ is an $n \times n$ diagonal matrix, independent of $\mathbf{X}$. Assume that, almost surely, as $n \to \infty$, $F^{\mathbf{T}}$ converges to a distribution function *H*, and the ratio $n/N \to c > 0$. Then, almost surely, $F^{(1/N)\mathbf{XTX}^H}$ converges to a nonrandom distribution function *G*. The Stieltjes transform m_G of *G* is the unique (pointwise) solution to

$$m(z) = \frac{1}{-z + c\int \frac{\tau}{1+\tau m(z)} dH(\tau)}, z \in C^+ . \tag{5}$$

For the special case of $\frac{1}{N}\mathbf{HH}^H$, where $\mathbf{H}$ is the channel matrix of our model, according to Theorem II.1, the Stieltjes transform of the limiting distribution is given by

$$m_G(z) = \frac{(-1+\beta-z)+\sqrt{-4z+(1+z-\beta)^2}}{2z} = -\frac{1}{z} - \frac{1}{4}\mathcal{F}\left(-\frac{1}{z}, \beta\right), \tag{6}$$

where

$$\mathcal{F}(x,z) \triangleq \left(\sqrt{x(1+\sqrt{z})^2+1} - \sqrt{x(1-\sqrt{z})^2+1}\right)^2 . \tag{7}$$

The limiting distribution admits a closed-form expression in this case, whose probability density function is given by

$$f_G(x) = [1-\beta]^+ \delta(x) + \frac{\sqrt{[x-a(\beta)]^+[b(\beta)-x]^+}}{2\pi x}, \tag{8}$$

where $\delta(x)$ is a unit point mass at 0, $[x]^+ = \max\{x, 0\}$, and $a(x) = (1-\sqrt{x})^2$, $b(x) = (1+\sqrt{x})^2$.

Similarly, $F^{(1/K)\mathbf{H}\,\mathbf{H}^H}$ converges to the distribution function of

$$f_{1/\beta}(x) = [1-\beta]^+ \delta(x) + \frac{\sqrt{[x-a\left(1/\beta\right)]^+[b\left(1/\beta\right)-x]^+}}{2\pi\left(1/\beta\right)x} . \tag{9}$$

III. Asymptotic Spectral Efficiency of Multicell MIMO Systems

For the single-cell model (1) with the associated assumptions, the optimum spectral efficiency is given by [13], [27]

$$C_{S-opt} = \log\det\left[\frac{\sigma^2\mathbf{I} + \frac{P}{K}\mathbf{HH}^H}{\sigma^2\mathbf{I}}\right] = \log\det\left[\mathbf{I} + \frac{\rho}{K}\mathbf{HH}^H\right]. \tag{10}$$

In the limiting region, we have the following

$$\lim_{N\to\infty}\frac{1}{N}C_{S-opt} = \lim_{N\to\infty}\frac{1}{N}\sum_{i=1}^{N}\log(1+\rho\lambda_i) = E\ \{\log(1+\rho\lambda)\}, \tag{11}$$

where $\{\lambda_i\}$ are the eigenvalues of $\frac{1}{K}\mathbf{H}\mathbf{H}^H$, whose limiting probability density function is given by (9). Note that $\mathcal{C}(x) = E\{\log(1+x\lambda)\}$ is an increasing function of x with $\mathcal{C}(0)=0$ and $\frac{d}{dx}\mathcal{C}(x) = \log e\cdot E\left\{\frac{\lambda}{1+x\lambda}\right\}$. So we can express (11) as

$$\lim_{N\to\infty}\frac{1}{N}C_{S-opt} = \log e\cdot\int_0^{\rho}E\left\{\frac{\lambda}{1+x\lambda}\right\}dx = \log e\cdot\int_0^{\rho}\frac{1}{x}\left(1-E\left\{\frac{1}{1+x\lambda}\right\}\right)dx. \tag{12}$$

$E\left\{\frac{1}{1+x\lambda}\right\}$ can be calculated explicitly as

$$\begin{aligned}
E\left\{\frac{1}{1+x\lambda}\right\} &= \int\frac{1}{1+x\lambda}f_{1/\beta}(\lambda)d\lambda \\
&= (1-\beta)+\int_{a\left(1/\beta\right)}^{b\left(1/\beta\right)}\frac{1}{1+x\lambda}\frac{\sqrt{[\lambda-a\left(1/\beta\right)][b\left(1/\beta\right)-\lambda]}}{2\pi\left(1/\beta\right)\lambda}d\lambda \\
&= (1-\beta)+\beta\int_{a(\beta)}^{b(\beta)}\frac{1}{1+\frac{x}{\beta}\omega}\frac{\sqrt{[\omega-a(\beta)][b(\beta)-\omega]}}{2\pi\beta\omega}d\omega \\
&= (1-\beta)+\beta\left(1-\frac{1}{4x}\mathcal{F}\left(\frac{x}{\beta},\beta\right)\right) \\
&= 1-\frac{\beta}{4x}\mathcal{F}\left(x/\beta,\beta\right),
\end{aligned} \tag{13}$$

where the second-to-last definite integral result is derived in [14], [32], and the function $\mathcal{F}(x,z)$ is given in (7). Finally,

$$\lim_{N\to\infty}\frac{1}{N}C_{S-opt} = \log e\cdot\int_0^{\rho}\frac{\beta}{4x^2}\mathcal{F}(x/\beta,\beta)dx = \log e\cdot\int_0^{\rho/\beta}\frac{1}{4y^2}\mathcal{F}(y,\beta)dy = \mathcal{G}(\rho/\beta,\beta), \tag{14}$$

with

$$\mathcal{G}(x,z) = z\log(1+x-\tfrac{1}{4}\mathcal{F}(x,z))+\log(1+xz-\tfrac{1}{4}\mathcal{F}(x,z))-\frac{\log e}{4x}\mathcal{F}(x,z), \tag{15}$$

where the last equality of (14) follows after some algebra.

Clearly, this interference-free theoretical limit is an upper bound for the achievable spectral efficiency of multicell MIMO systems. In the following subsections, we give the spectral efficiencies of multicell MIMO systems with several detectors of interest.

A. Joint Optimum Detector

The joint optimum detector assumes that the receiver knows the signaling and channel information of other cells and performs joint detection. In this situation, model (3) describes a multiple-access channel [7]. For the Gaussian multiple access channel, the capacity region is specified in [30] as (couched in the notation of the present paper)

$$\bigcap_{I\subset\{1,\ldots,K(L+1)\}} \{(R_1,\ldots,R_{K(L+1)}) : 0 \le \sum_{i\in I} R_i \le \log\det[\mathbf{I}+\frac{\rho}{K}(\mathbf{H}_E)_I(\mathbf{H}_E)_I{}^H]\}\,, \tag{16}$$

where

$$\mathbf{H}_E = [\mathbf{H}, \alpha_1\mathbf{H}_{if1},\ldots,\alpha_L\mathbf{H}_{ifL}]\,, \tag{17}$$

and $(\mathbf{H}_E)_I$ denotes the $N\times|I|$ submatrix of $\mathbf{H}_E$ obtained by striking out the columns whose indices do not belong to *I*, with $|I|$ the cardinality of *I*. Here $R_1,\ldots,R_K$ denote the data rates of the substreams of the MIMO system in the desired cell, $R_{K+1},\ldots,R_{2K}$ refer to those of the first interfering cell with attenuation factor α_1, and so on. The following proposition is a specific application of (16).

Proposition III.1: The sum spectral efficiency of the set of cells of interest (cell 0 is the desired cell) $J\subset\{0,1,\ldots,L\}$ with the joint optimum detector, assuming no interference from the cells in $\bar{J}$ (the complement of *J* in $\{0,1,\ldots,L\}$) [5]is

$$SR_{M-opt}^{(J)} = \log\det\left[\mathbf{I}+\frac{\rho}{K}(\mathbf{H}_E)_J(\mathbf{H}_E)_J{}^H\right], \tag{18}$$

where $(\mathbf{H}_E)_J$ means the $N\times|J|K$ submatrix of $\mathbf{H}_E$ obtained by striking out the channel matrices of the cells whose indices do not belong to *J*. Specifically, the sum spectral efficiency of all $L+1$ cells with the joint optimum detector is given by

$$SR_{M-opt}^{\{0,1,\ldots,L\}} = \log\det\left[\mathbf{I}+\frac{\rho}{K}(\mathbf{H}_E)(\mathbf{H}_E)^H\right].$$

[5] This can arise, e.g., in the scenario when there are no active users in the cells of $\bar{J}$, or when interference from the cells in $\bar{J}$ are assumed to be cancelled out perfectly (see lemma III.1). The expression of (18) together with its asymptotic analysis will be used to facilitate the calculation of the asymptotic spectral efficiencies of other detectors in the following.

In the limit, we can rewrite (18) as

$$\begin{aligned}\lim_{N\to\infty}\frac{1}{N}SR^{(J)}_{M-opt} &= \lim_{N\to\infty}\frac{1}{N}\log\det\left[\mathbf{I}+\frac{\rho}{K}(\mathbf{H}_E)_J(\mathbf{H}_E)_J{}^H\right]=\lim_{N\to\infty}\frac{1}{N}\log\det\left[\mathbf{I}+\frac{\rho}{\beta}\frac{1}{N}(\mathbf{H}_E)_J(\mathbf{H}_E)_J{}^H\right]\\ &= \lim_{N\to\infty}\frac{1}{N}\sum_{i=1}^{N}\log\left(1+\frac{\rho}{\beta}\lambda_i\right)=E\left\{\log\left(1+\frac{\rho}{\beta}\lambda\right)\right\},\end{aligned} \tag{19}$$

where $\{\lambda_i\}$ are the eigenvalues of

$$\frac{1}{N}(\mathbf{H}_E)_J(\mathbf{H}_E)_J{}^H=\frac{1}{N}[\mathbf{H}_{i_1},\ldots,\mathbf{H}_{i_{|J|}}]\begin{bmatrix}\alpha^2_{i_1} & & \\ & \ddots & \\ & & \alpha^2_{i_{|J|}}\end{bmatrix}[\mathbf{H}_{i_1},\ldots,\mathbf{H}_{i_{|J|}}]^H . \tag{20}$$

Note that (20) conforms with the conditions of Theorem II.1, so the empirical eigenvalue distribution of $\frac{1}{N}(\mathbf{H}_E)_J(\mathbf{H}_E)_J{}^H$ converges to a nonrandom distribution function *Q*, whose Stieltjes transform $m_Q(z)$ is a unique solution to

$$m_Q(z)=\frac{1}{-z+|J|\beta\int\frac{\tau}{1+\tau m_Q(z)}dH(\tau)}=\frac{1}{-z+\beta\sum_{j=1}^{|J|}\frac{\alpha^2_{i_j}}{1+\alpha^2_{i_j}m_Q(z)}} \tag{21}$$

By (4), we have

$$m_Q(z)=E\left\{\frac{1}{\lambda-z}\right\}. \tag{22}$$

So

$$E\left\{\frac{\lambda}{1+x\lambda}\right\}=\frac{x-m_Q\left(-\frac{1}{x}\right)}{x^2}. \tag{23}$$

Therefore, using the same differentiation-integration strategy as (12), we have

$$\lim_{N\to\infty}\frac{1}{N}SR^{(J)}_{M-opt}=\log e\cdot\int_0^{\rho/\beta}\frac{x-m_Q\left(-\frac{1}{x}\right)}{x^2}dx , \tag{24}$$

where $m_Q(x)$ is an implicit solution of (21).

The exact formula (24) requires numerical fixed-point solutions of (21) and computation of the definite integral of (24), which is fairly complex. So, an approximation of (18) in the limiting region is explored here. The idea is to approximate $(\mathbf{H}_E)_J(\mathbf{H}_E)_J{}^H$ as

$$(\mathbf{H}_E)_J(\mathbf{H}_E)_J{}^H \approx \frac{\sum_{i\in J}\alpha_i^2}{|J|}\mathbf{H}'(\mathbf{H}')^H\,, \tag{25}$$

where $\mathbf{H}'$ denotes an $N \times K|J|$ random matrix with i.i.d. normalized complex Gaussian entries. In this way, a closed-form formula similar to (14) can be obtained. Note that even though we assume $\beta \le 1$ throughout the paper, we should discern here whether $\beta \le 1/|J|$, which determines whether the empirical eigenvalue distribution of $\frac{1}{K|J|}\mathbf{H}'(\mathbf{H}')^H$ has a mass point at 0 (see (9)). Finally, we get the following approximate formula for (24), which *holds* for all values of $\beta \in (0,1]$:

$$\lim_{N\to\infty}\frac{1}{N}SR_{M-opt}^{(J)} \approx \beta|J|G\left(\rho\sum_{i\subset J}\alpha_i^2,\, 1/\beta|J|\right) = G\left(\frac{\rho\sum_{i\subset J}\alpha_i^2}{\beta|J|},\beta|J|\right). \tag{26}$$

We will see in the following that (26) gives a good approximation for a wide range of parameter settings. It tends to overestimate when β is small or there is great discrepancy within the set of $\{\alpha_i\}$ of interest. Even in this case, (26) roughly exhibits the same behavior as (24), and thus is still useful for theoretical analysis.

B. Group Linear MMSE Detector

While approaching the optimum performance, joint maximum likelihood detection for multicell MIMO systems is impractical for most current applications due to its complexity [8]. With no intention of detecting the data from the interfering cells, group linear MMSE MUD is one of the most favorable techniques to suppress the intercell interference. The detection process is to first apply the weight matrix

$$\mathbf{W} = \left(\mathbf{H}\mathbf{H}^H + \sum_i \alpha_i^2\mathbf{H}_{ifi}\mathbf{H}_{ifi}{}^H + \frac{K}{\rho}\mathbf{I}\right)^{-1}\mathbf{H} \tag{27}$$

to the received signal (3) to combat the intercell interference, and then to *optimally* detect the data of the desired cell. The following result has been proved in [8].

Proposition III.2: The multicell spectral efficiency of the desired-cell MIMO system with the group linear MMSE detector is given asymptotically as[6]

$$C_{M-mmse} \sim \log\det[\mathbf{I} + \frac{P}{K}\mathbf{H}\mathbf{H}^H\mathbf{\Sigma}^{-1}]\,, \tag{28}$$

---

[6] Here, $X \sim Y$ means that $\lim_{N\to\infty}\frac{X}{Y} = 1$.

where

$$\mathbf{\Sigma} = \sum_{i=1}^{L} \alpha_i^2 \frac{P}{K} \mathbf{H}_{ifi} \mathbf{H}_{ifi}{}^H + \sigma^2 \mathbf{I} \,. \tag{29}$$

From Proposition III.2, we have the following consequence.

Corollary III.1: The multicell spectral efficiency of the desired-cell MIMO system with the group linear MMSE detector is asymptotically related to the sum spectral efficiency of the multicell MIMO systems with the joint optimum detector given in (18) as

$$C_{M-mmse} \sim SR_{M-opt}^{\{0,1,\ldots,L\}} - SR_{M-opt}^{\{1,\ldots,L\}} \,. \tag{30}$$

Proof: By (29),

$$\mathbf{\Sigma} = \sum_{i=1}^{L} \alpha_i^2 \frac{P}{K} \mathbf{H}_{ifi} \mathbf{H}_{ifi}{}^H + \sigma^2 \mathbf{I} = \frac{P}{K} (\mathbf{H}_E \mathbf{H}_E{}^H - \mathbf{H}\mathbf{H}^H) + \sigma^2 \mathbf{I}.$$

So,

$$\frac{\rho}{K} (\mathbf{H}_E \mathbf{H}_E{}^H - \mathbf{H}\mathbf{H}^H) = \frac{1}{\sigma^2} \mathbf{\Sigma} - \mathbf{I} \,,$$

and

$$\frac{\rho}{K} \mathbf{H}_E \mathbf{H}_E{}^H = \frac{\rho}{K} \mathbf{H}\mathbf{H}^H + \frac{1}{\sigma^2} \mathbf{\Sigma} - \mathbf{I} \,.$$

Therefore,

$$\mathbf{I} + \frac{P}{K} \mathbf{H}\mathbf{H}^H \mathbf{\Sigma}^{-1} = \frac{\mathbf{I} + \frac{\rho}{K} \mathbf{H}_E \mathbf{H}_E{}^H}{\mathbf{I} + \frac{\rho}{K} (\mathbf{H}_E \mathbf{H}_E{}^H - \mathbf{H}\mathbf{H}^H)} \,. \tag{31}$$

On comparing (18) and (28), (30) follows.

□

With (30) and (26), we readily have

$$\lim_{N \to \infty} \frac{1}{N} C_{M-mmse} \approx G\left(\frac{\rho(1+1/\mu)}{\beta(L+1)}, \beta(L+1) \right) - G\left(\frac{\rho(1/\mu)}{\beta L}, \beta L \right). \tag{32}$$

In general, if we partition the cells into two groups, applying the linear MMSE detector to one of them to suppress the interference from the other, followed by *optimal* detection within the set of cells of interest, the sum spectral efficiency is exactly analogous to (30). Thus, we have the following.

Corollary III.2: The sum spectral efficiency of the set of cells of interest (cell 0 is the desired cell) $J \subset \{0,1,\ldots,L\}$ with the *generalized* group linear MMSE detector is given asymptotically as

$$SR_{M-gmmse}^{(J)} \sim SR_{M-opt}^{\{0,1,\ldots,L\}} - SR_{M-opt}^{(\bar{J})}, \tag{33}$$

where $\bar{J}$ is the complement of J in $\{0,1,\ldots,L\}$.

Comments: Note that $SR_{M-gmmse}^{\{0\}} = C_{M-mmse}$, while $SR_{M-gmmse}^{\{0,1,\ldots,L\}} = SR_{M-opt}^{\{0,1,\ldots,L\}}$. Within the set J of cells of interest, while treating the interference from other cells in $\bar{J}$ as Gaussian background noise (due to MMSE processing), we can similarly define a multiple access capacity region as in Proposition III.1 (note that we assume *optimal* detection within the set J of cells of interest). Denote a set $K \subset J$; then the sum spectral efficiency of the set K is bounded asymptotically by[7]

$$SR_{M-gmmse}^{(J,K)} \prec \log\det\left[\mathbf{I} + \frac{P}{K}(\mathbf{H}_E)_K(\mathbf{H}_E)_K{}^H \mathbf{\Sigma}_{\bar{J}}^{-1}\right] = SR_{M-opt}^{(K\cup\bar{J})} - SR_{M-opt}^{(\bar{J})}, \tag{34}$$

where $\mathbf{\Sigma}_{\bar{J}} = \sum_{i\in\bar{J}} \alpha_i^2 \frac{P}{K}\mathbf{H}_{ifi}\mathbf{H}_{ifi}{}^H + \sigma^2\mathbf{I}$.

C. Group MMSE Successive Interference Cancellation Detector

Since joint maximum likelihood detection for multicell MIMO systems is highly complex, while linear MMSE MUD is limited in its interference cancellation capability, suboptimum non-linear multiuser detection often provides a favorable tradeoff between performance and complexity (see, e.g., [21]). Group MMSE successive interference cancellation is one such technique, in which information symbols are detected by group linear MMSE detection cell by cell, with the interference from previously detected cells already being subtracted. Although successive interference cancellation does not result in maximum-likelihood decisions, it becomes asymptotically optimal as the error probability of intermediate decisions vanishes with code block length [29]. With the assumption of perfect cancellation, the following lemma shows the optimality of group MMSE successive interference cancellation.

Lemma III.1: Assuming perfect cancellation of interference from previous detected cells, the group MMSE successive interference cancellation detector asymptotically achieves one of the vertices of the capacity region given by (34).

---

[7] Here, $X \prec Y$ means that $\lim_{N\to\infty} \frac{X}{Y} \le 1$.

Proof: Suppose the group MMSE successive interference cancellation detector is applied to the set of cells of interest $J=\{i_1,\ldots,i_{|J|}\}\subset\{0,1,\ldots,L\}$. Without loss of generality, also suppose the cells are detected in that order. Following Corollary III.1, and assuming perfect cancellation of the interference from the detected cells, we have

$$C_{M-sic}^{(i_1)} \sim SR_{M-opt}^{\{0,1,\ldots,L\}} - SR_{M-opt}^{\{0,1,\ldots,L\}\backslash\{i_1\}},$$

$$C_{M-sic}^{(i_2)} \sim SR_{M-opt}^{\{0,1,\ldots,L\}\backslash\{i_1\}} - SR_{M-opt}^{\{0,1,\ldots,L\}\backslash\{i_1,i_2\}},$$

$$\vdots$$

$$C_{M-sic}^{(i_{|J|})} \sim SR_{M-opt}^{\{0,1,\ldots,L\}\backslash\{i_1,\ldots,i_{|J|-1}\}} - SR_{M-opt}^{\{0,1,\ldots,L\}\backslash J}. \tag{35}$$

Equivalently, the above $|J|$ equalities can be reformulated as

$$SR_{M-sic}^{(J,\{i_{|J|}\})} = C_{M-sic}^{(i_{|J|})} \sim SR_{M-opt}^{\{i_{|J|}\}\cup\bar{J}} - SR_{M-opt}^{(\bar{J})},$$

$$SR_{M-sic}^{(J,\{i_{|J|-1},i_{|J|}\})} = C_{M-sic}^{(i_{|J|-1})} + C_{M-sic}^{(i_{|J|})} \sim SR_{M-opt}^{\{i_{|J|-1},i_{|J|}\}\cup\bar{J}} - SR_{M-opt}^{(\bar{J})},$$

$$\vdots$$

$$SR_{M-sic}^{(J)} = C_{M-sic}^{(i_1)} + \cdots + C_{M-sic}^{(i_{|J|-1})} + C_{M-sic}^{(i_{|J|})} \sim SR_{M-opt}^{\{0,1,\ldots,L\}} - SR_{M-opt}^{(\bar{J})}. \tag{36}$$

On comparing (36) with (34), we see that one of the vertices of the Gaussian multiple access capacity region is achieved.

□

Comments: When the group MMSE successive interference cancellation is applied to a subgroup $J\subset\{0,1,\ldots,L\}$, we could first apply the generalized group linear MMSE detector to the received signal to get an estimate for the data of interest (corresponding to the chosen subgroup). Then based on this estimate, we could further apply the group MMSE successive interference cancellation. That is, we could carry out the MMSE filtering in two steps. It can be shown that this two-step MMSE filtering is equivalent to the one-step MMSE filtering adopted here. To see this, let us denote the MMSE filters employed in the two-step case by $\mathbf{W}_1$ and $\mathbf{W}_2$, and denote the one employed in our approach by $\mathbf{W}$. By the orthogonality principle, we have $E\{(\mathbf{x}_J-\mathbf{W}_1^H\mathbf{y})\mathbf{y}^H\mathbf{W}_1\}=\mathbf{0}$, $E\{(\mathbf{x}_j-\mathbf{W}_2^H(\mathbf{W}_1^H\mathbf{y}))\mathbf{y}^H\mathbf{W}_1\mathbf{W}_2\}=\mathbf{0}$, and $E\{(\mathbf{x}_j-\mathbf{W}^H\mathbf{y})\mathbf{y}^H\mathbf{W}\}=\mathbf{0}$, where $\mathbf{x}_J$ refers to the group of data of interest (collected into a $|J|K\times 1$ vector), and $\mathbf{x}_j$, $j\in J$ refers to one of them. Clearly we have $\mathbf{W}=\mathbf{W}_1\mathbf{W}_2$. As the group MMSE successive interference cancellation detector has $|J|!$ different orders of detection, $|J|!$ vertices of the capacity region in the $R^{|J|}$ domain can be achieved. As the capacity region of the multiple-access channel is convex, by timesharing, the group MMSE successive interference cancellation detector can thus achieve the capacity region spanned by these vertices.

From Lemma III.1, we have the following corollary.

Corollary III.3:

$$SR^{(J)}_{M-sic} = \sum_{i \in J} C^{(i)}_{M-sic} = SR^{(J)}_{M-gmmse} \sim SR^{\{0,1,\ldots,L\}}_{M-opt} - SR^{(\bar{J})}_{M-opt} , \tag{37}$$

$$SR^{\{0\}}_{M-sic} = SR^{\{0\}}_{M-gmmse} = C_{M-mmse} , \tag{38}$$

and

$$SR^{\{0,1,\ldots,L\}}_{M-sic} = SR^{\{0,1,\ldots,L\}}_{M-gmmse} = SR^{\{0,1,\ldots,L\}}_{M-opt} . \tag{39}$$

To achieve some vertex of the capacity region of the Gaussian multiple access channel that corresponds to the maximum rate for the desired cell (single cell capacity), Lemma III.1 suggests a detection order that puts the detection of the desired cell last. For example, when the cells are detected in the order of $\{L, L-1, \ldots, 0\}$, the achieved capacity vertex is given by $(R^{(L)}_{M-sic}, \ldots, R^{(1)}_{M-sic}, R^{(0)}_{M-sic})$ with

$$R^{(l)}_{M-sic} \sim SR^{\{0,1,\ldots,l\}}_{M-opt} - SR^{\{0,1,\ldots,l-1\}}_{M-opt} , \quad l = L, \ldots, 1 \tag{40}$$

and

$$R^{(0)}_{M-sic} \sim SR^{\{0\}}_{M-opt} = C_{S-opt} . \tag{41}$$

Note that, in practice, the success of interference cancellation relies heavily on the correct detection of interference. In adverse environments where we cannot get good estimates of interference, successive interference cancellation schemes will worsen the performance instead of improving it [8]. Therefore, to achieve the optimal capacity of (41), MMSE successive interference cancellation implicitly requires that the data rates of other interfering cells satisfy (40). This is impractical, as it requires not only joint signaling but also puts the desired cell in a superior position. What is of practical interest is that all cells are autonomous with identical data rates. This identical rate-tuple can in general be achieved by time sharing. With this restriction, the following proposition shows the limitations of the group MMSE successive interference cancellation detector.

Proposition III.3: Assuming that the same data rate is employed in each cell, and that $0 \le \alpha_L \le \cdots \le \alpha_1 \le 1$, the multicell spectral efficiency of the desired-cell MIMO system with the group MMSE successive interference cancellation detector applied to the cells $J = \{0,1,\ldots,l\}$ is given asymptotically as

$$C_{M-sic}^{(l)} \sim \min_{k=1,\ldots,l+1} \left(\frac{SR_{M-opt}^{\{l-k+1,\ldots,L\}} - SR_{M-opt}^{\{l+1,\ldots,L\}}}{k} \right), l = 0,1,\ldots,L \,. \tag{42}$$

Proof: For any fixed $l \in \{1,\ldots,L\}$, assume that the same data rate is employed in each cell, i.e., $R_{M-sic}^{(i)} = R^{(l)}, \quad i = 0,1,\ldots,l$. We then have

$$SR_{M-sic}^{(J,K)} = \left|K\right| R^{(l)} , \tag{43}$$

for a given set $K \subset J$. The above sum rate of cells in set *K* is bounded by the multiple access capacity region given in (34) as

$$\left|K\right| R^{(l)} \prec SR_{M-opt}^{(K \cup \bar{J})} - SR_{M-opt}^{(\bar{J})} . \tag{44}$$

Due to the condition $0 \le \alpha_L \le \cdots \le \alpha_1 \le 1$, we can rule out most of the constraints. We claim that for a given |*K*|, when $N \to \infty$,

$$\min_{K} \left(SR_{M-opt}^{(K \cup \bar{J})} - SR_{M-opt}^{(\bar{J})} \right) = SR_{M-opt}^{\{l-|K|+1,\ldots,L\}} - SR_{M-opt}^{(\bar{J})} , \tag{45}$$

i.e., the sum rate of cells corresponding to the largest attenuations has the strictest constraint. This claim is proved in Appendix I. Therefore, we have

$$R^{(l)} \prec \frac{SR_{M-opt}^{\{l-|K|+1,\ldots,L\}} - SR_{M-opt}^{\{l+1,\ldots,L\}}}{|K|} , \tag{46}$$

for all $1 \le |K| \le |J| = 1 + l$, and thus

$$R^{(l)} \prec \min_{k=1,\ldots,l+1} \left(\frac{SR_{M-opt}^{\{l-k+1,\ldots,L\}} - SR_{M-opt}^{\{l+1,\ldots,L\}}}{k} \right) . \tag{47}$$

We learn from Lemma III.1 that different orders of the group MMSE successive interference cancellation achieve different vertices of the multiple access capacity region expressed in (34), and the identical rate-tuple can be achieved by time sharing of different detection orders. Therefore, the rate on the right hand side of (47) is achievable. We then have

$$C_{M-sic}^{(l)} = \min_{k=1,\ldots,l+1} \left(\frac{SR_{M-opt}^{\{l-k+1,\ldots,L\}} - SR_{M-opt}^{\{l+1,\ldots,L\}}}{k} \right), \tag{48}$$

for $l \in \{1,\ldots,L\}$. Noting that $C_{M-sic}^{(0)} = C_{M-mmse}$, (42) follows readily.

□

Comments: Note that to jointly detect $l+1$ cells, including cell 0, the set $J = \{0,1,\ldots,l\}$ is optimal, as any other choice can only lower the capacity (42) due to the condition $0 \le \alpha_L \le \cdots \le \alpha_1 \le 1$.

D. Adaptive Multiuser Detector

From Proposition III.3, we see that the group MMSE successive interference cancellation detector is not necessarily better than the simpler group linear MMSE detector. Likewise, it is not always better to try to detect more cells. These observations are confirmed in [8]. An (ideal) adaptive detector will always assume the best performance among linear MMSE MUD and various partial or full interference cancellation detectors. This detector can be approximated by a receiver that chooses different detection schemes according to some thresholds determined by experiments [8]. For this idealized multicell detector, we have the following result.

Proposition III.4: The multicell spectral efficiency of the desired cell MIMO system with the adaptive multiuser detector is

$$C_{M-adpt} = \max_{l=0,\ldots,L} C_{M-sic}^{(l)}. \tag{49}$$

IV. Some Analytical and Numerical Results

In this section, some analytical and numerical results are given as applications of the above derived formulas, from which we can gain some insights into the behavior of multicell MIMO systems. Unless otherwise specified, we assume a multicell model having four interferers in two groups of two, in which one group is 6 dB stronger than the other while the users within each group have the same power. This roughly reflects the essential reality of one-tier hexagonal cellular structure, as interference from the two farthest adjacent cells can typically be ignored, and simulation results verify that the power of the two strongest users usually dominates [8]. Therefore, we assume the following parameters for (3): $L = 4$, and

$$\alpha_1^2 = \frac{1}{\mu}\frac{\gamma}{1+\gamma}\frac{\beta_1}{1+\beta_1}, \alpha_2^2 = \frac{1}{\mu}\frac{\gamma}{1+\gamma}\frac{1}{1+\beta_1}, \alpha_3^2 = \frac{1}{\mu}\frac{1}{1+\gamma}\frac{\beta_2}{1+\beta_2}, \alpha_4^2 = \frac{1}{\mu}\frac{1}{1+\gamma}\frac{1}{1+\beta_2}, \tag{50}$$

with $\gamma = 4$, $\beta_1 = 1$, and $\beta_2 = 1$. Recall that μ is the SIR. Further, as spectral efficiencies of MIMO systems grow linearly with the number of receive antennas *N*, in our study we are mainly interested in normalized spectral efficiencies per receive antenna. The reader should keep this in mind when interpreting the overall MIMO capacity from the following figures.

In the following, a single-cell detector is sometimes referred to for comparison. This detector treats intercell interference as additive white Gaussian noise (AWGN), so its spectral efficiency C_{M-s} is of the same form as (10), with the noise spectral height replaced by $\sigma^2 + P\sum_{i=1}^{L}\alpha_i^2 = \sigma^2(1+\rho/\mu)$. In the limiting region we have

$$\lim_{N\to\infty}\frac{1}{N}C_{M-s} = G\left(\rho \big/ (1+\rho/\mu)\beta, \beta\right). \quad (51)$$

In [8], the performance of a turbo space-time multiuser detector in the interference-limited multicell situation wasexamined, where exactly the same approximation (AWGN) for intercell interference was made. It was shown that in the single-cell scenario, this turbo space-time multiuser detector very closely approaches the single-cell capacity, while in the interference-limited multicell scenario, its performance is greatly degraded, and multiuser detection across the cell can significantly improve the system performance. Therefore, (51) can be viewed as a guideline for the performance of this turbo space-time multiuser detector in the interference-limited multicell scenario. The reader is referred to [35] and [4] for similar and alternative approaches on this topic.

A. Interference-Limited Behavior

Clearly, the single-cell detector of (51) is interference limited, which can be verified through

$$\lim_{\rho\to\infty} G\left(\rho \big/ (1+\rho/\mu)\beta, \beta\right) = G\left(\mu \big/ \beta, \beta\right). \quad (52)$$

Evn though for $\beta = 1$, the group linear MMSE detector was also found to be interference limited [8], we noted that this is due to the lack of sufficient degrees of freedom at the receiver to suppress the co-channel interference. We believe that if β is sufficiently small, the group linear MMSE detector is *not* interference limited. This is verified in Figs. 1 (a)-(c). Here the SIR is set to be 0 dB, indicating a strong interference environment. It is observed in these figures that the spectral efficiency of the single cell upper bound (see (14)) and that of the single-cell detector (see (51)) decrease as the system load β decreases. The single-cell detector is interference-limited, with the limiting value given by (52). The spectral efficiency of the group linear MMSE detector, both the exact (see (30) and (24)) and the approximate (see (32)), however, increases as

β decreases, when the SNR is sufficiently large[8]. Furthermore, when the system load decreases to 1/5, the group linear MMSE detector is not interference limited. Comparing Figs. 1(a), Fig. 1(c) with Fig. 1 (d), where a more favorable SIR = 5 dB is experienced, we can see that all the multicell spectral efficiencies increase as SIR increases. However, due to the interference-limited nature, the spectral efficiency of the group linear MMSE detector with system load 1 is outperformed by the same detector with system load 1/5 at a much worse SIR, when the SNR is sufficiently large. This observation is helpful for multicell MIMO system design. Finally, we observe that the approximate formula well matches the exact one, thus providing a valuable tool for analysis.

Let us turn to the normalized approximate formula for the group linear MMSE detector, given as

$$\lim_{N\to\infty} C_{M-mmse}/N \approx R(\rho,\mu,\beta) \triangleq G\left(\frac{\rho(1+1/\mu)}{\beta(L+1)},\beta(L+1)\right) - G\left(\frac{\rho(1/\mu)}{\beta L},\beta L\right), \tag{53}$$

to study the interference-limited behavior of the group linear MMSE detector. In Appendix II, we show that

$$\lim_{\rho\to\infty} R(\rho,\mu,\beta) = \log(1+\mu) + (1-\beta(L+1))\log\left(1-\frac{1}{\beta(L+1)}\right) + (\beta L-1)\log\left(1-\frac{1}{\beta L}\right) \quad \text{when} \quad \beta > \frac{1}{\mathrm{L}}, \tag{54}$$

and

$$\lim_{\rho\to\infty} R(\rho,\mu,\beta) = \infty \quad \text{when} \quad \beta \le \frac{1}{\mathrm{L}+1}. \tag{55}$$

The analytical results of (54) and (55) agree with the numerical results of Fig. 1 very well. Thus the "magic" number 1/5 is not found by chance but rather is determined by the system behavior.

B. Adaptive Detection

We continue to study the behavior of the group MMSE successive interference cancellation detector (see (42)) and the adaptive multiuser detector (see (49)). The asymptotic spectral efficiencies given in this subsection are calculated with the exact formula (24). In the following figures, we use "Group MMSE SC-l" to denote the multicell spectral efficiency of the desired MIMO system with the group MMSE successive interference cancellation detector applied to the cells $J=\{0,1,\ldots,l-1\}$. The group linear MMSE detector corresponds to "Group MMSE SC-1", and the adaptive detector achieves the best among these detectors.

From Figs. 2 (a) and (b) we see that, for a fairly high SIR (5dB), the simpler group linear MMSE detector is the best; but in a strong interference environment (0 dB), group MMSE successive interference cancellation proves to be useful. This

[8] For a fixed SNR, there is an optimal β for the linear MMSE detector for the single cell case (see [32]).

verifies the well-known fact that detection of the interfering users is optimal only in the strong-interference case; for weak interference, it is better to simply treat the interference as ambient noise. It is also observed that, in the scenario of sufficiently high SNR, the group MMSE successive interference cancellation detector applied to all the cells eventually stands out, but for other cases, trying to detect more cells actually lowers the possible achieved capacity. This is more evident in Fig. 2 (c), where a one-dominant-interferer scenario with $\gamma = 3.5, \beta_1 = 6, \beta_2 = 1$ (the power of the strongest interferer is 3 dB higher than the power sum of the remaining interferers) is assumed. We find that for low to medium SNR, detection of only the strongest interferer is the best, while the MMSE successive interference cancellation applied to all the cells is the best in the high SNR regime.

In Fig. 3 (a), we show the spectral efficiencies of the ideal adaptive detector for different SNR and SIR scenarios. We assume the model of (50) with $\gamma = 4, \beta_1 = 1, \beta_2 = 1$, and system load 1. We also show the single cell upper bound and the spectral efficiencies of the single-cell detector for reference. We see that multiuser detection across the cell is most useful in the strong interference environment. Its advantage over the single-cell detector diminishes as SIR increases. In the strong interference environment, even though multiuser detection across the cell brings substantial gain over single-cell detection, there is a substantial gap between the achievable capacity and the single cell upper bound. These observations are not true for sufficiently low system load, as is shown in Fig. 3(b). There we see that multiuser detection across the cell is useful in all interference environments, and MUD capacity approaches the single cell upper bound quite well. However, as the system load is reduced, the achievable capacity is also reduced. Therefore, there is a tradeoff among system load, energy, receiver complexity and achievable capacity for multicell MIMO system design.

V. Conclusions

In this paper, we have studied the spectral efficiencies of multicell MIMO systems with several multiuser detectors. The large-system asymptotic (non-random) expressions for these spectral efficiencies have also been explored. Simple relationships have been found among these capacity formulas, and all of them can be well approximated with standard functions, which makes theoretical analysis of multicell MIMO systems more expedient.

As applications of these theoretical bounds, we have verified the following results from [8] about multicell MIMO systems. Group linear MMSE detection and group MMSE successive interference cancellation are two effective techniques to combat co-channel interference, each of which may outperform the other for different settings. Based on this observation, an adaptive detector was explored to attempt to achieve the better performance of the two. For full system load, multiuser detection across the cell is most useful in strong interference environments, offering substantial gain over traditional single-cell detectors. However, there is still a substantial gap between the achievable capacity and the single cell upper bound in this case.

Further, conditions for non-interference-limited behavior of the group linear MMSE detector have been found. Based on this result, it is suggested that with sufficiently low system load $\beta \le \frac{1}{L+1}$, where L is the number of effective interfering cells, better performance than that of the fully loaded system may be attained in the strong interference environment with sufficiently large signal power.

Acknowledgment: The authors would like to thank Prof. R. S. Blum and the anonymous reviewers for their helpful comments and suggestions.

Appendix I: Proof of Claim in Proposition III.3

First let us consider the fixed point solution given in (21). For any $z < 0$, let $x = m_Q(z)$ and define a function

$$h(x) == \frac{1}{-z + \beta \sum_{j=1}^{|K|} \frac{\alpha_{i_j}^2}{1+\alpha_{i_j}^2 x} + \beta \sum_{j=l+1}^{L} \frac{\alpha_j^2}{1+\alpha_j^2 x}} \quad (56)$$

Following an approach similar to that of Proposition 3.2 of [28], it can be shown that the function

$$f(x) \triangleq \frac{x}{h(x)} = (-z)x + \beta \sum_{j=1}^{|K|} \frac{\alpha_{i_j}^2 x}{1+\alpha_{i_j}^2 x} + \beta \sum_{j=l+1}^{L} \frac{\alpha_j^2 x}{1+\alpha_j^2 x} \quad (57)$$

is a continuous, strictly increasing function for $z < 0$. It can also be shown that $x = h(x)$ has a unique fixed point $x^* > 0$, corresponding to $f(x^*) = 1$, and for any x, $x \ge x^*$ if and only if $x \ge h(x)$ (corresponding to $f(x) \ge 1$).

Now let us consider two sets $K_1, K_2 \subset J = \{0,1,\ldots,l\}$ with $|K_1| = |K_2| = |K|$, $\alpha_{K_{11}}^2 \ge \alpha_{K_{12}}^2 \cdots \ge \alpha_{K_{1|K|}}^2$, and $\alpha_{K_{2j}}^2 = \alpha_{l-|K|+j}^2$, $j = 1,\ldots,|K|$. Clearly, we have

$$\alpha_{K_{1j}}^2 \geq \alpha_{K_{2j}}^2, \quad j = 1, \ldots, |K|. \tag{58}$$

Denote

$$h_i(x) == \frac{1}{-z + \beta \sum_{j=1}^{|K|} \frac{\alpha_{K_{ij}}^2}{1 + \alpha_{K_{ij}}^2 x} + \beta \sum_{j=l+1}^{L} \frac{\alpha_j^2}{1 + \alpha_j^2 x}} \tag{59}$$

for i = 1, 2. Let $x_i^* = h_i(x_i^*)$ for i = 1, 2, for any $z < 0$. Then we have

$$x_2^* = h_2(x_2^*) \geq h_1(x_2^*), \tag{60}$$

with the fact that

$$\frac{\alpha_{K_{1j}}^2}{1 + \alpha_{K_{1j}}^2 x} \geq \frac{\alpha_{K_{2j}}^2}{1 + \alpha_{K_{2j}}^2 x} \tag{61}$$

for $j = 1, \ldots, |K|$. Therefore, we conclude from (60) that

$$x_2^* = m_{Q2}(z) \geq x_1^* = m_{Q1}(z) \tag{62}$$

for every $z < 0$. Reflecting on (24), it is readily shown that

$$SR_{M-opt}^{(K_1 \cup \bar{J})} \succ SR_{M-opt}^{(K_2 \cup \bar{J})}, \tag{63}$$

and (45) follows.

This claim can also be verified through the approximate formula (26). Note that the function $G(x, z)$ defined in (15) is a strictly increasing function of x, as

$$\frac{\partial}{\partial x} G(x, z) = \frac{F(x, z)}{4x^2} > 0. \tag{64}$$

Appendix II: Derivation of Equations (54) and (55)

First let us examine the limiting behavior of the three parts of $G(x, z)$ in (15):

$$\lim_{x \to \infty} \frac{F(x, z)}{4x} = \min(z, 1), \tag{65}$$

$$\lim_{x \to \infty} 1 + x - \tfrac{1}{4} F(x, z) = \lim_{x \to \infty} \frac{1}{1 - F(x, z)/4zx} = \frac{1}{1 - \min(z, 1)/z}, \tag{66}$$

$$\lim_{x\to\infty} 1 + xz - \tfrac{1}{4}F(x,z) = \lim_{x\to\infty} \frac{1}{1 - F(x,z)\big/4x} = \frac{1}{1-\min(z,1)} . \tag{67}$$

We see that when $z \le 1$, (66) goes to infinity, and when $z \ge 1$, (67) goes to infinity.

Expanding (53), we have

$$R(\rho,\mu,\beta) = R_1(\rho,\mu,\beta) + R_2(\rho,\mu,\beta) + R_3(\rho,\mu,\beta) , \tag{68}$$

where

$$R_1(\rho,\mu,\beta) = -\log e\left(\frac{F(x_1,z_1)}{4x_1} - \frac{F(x_2,z_2)}{4x_2}\right), \tag{69}$$

$$R_2(\rho,\mu,\beta) = z_1 \log(1 + x_1 - \tfrac{1}{4}F(x_1,z_1)) - z_2 \log(1 + x_2 - \tfrac{1}{4}F(x_2,z_2)) , \tag{70}$$

and

$$R_3(\rho,\mu,\beta) = \log(1 + x_1 z_1 - \tfrac{1}{4}F(x_1,z_1)) - \log(1 + x_2 z_2 - \tfrac{1}{4}F(x_2,z_2)) , \tag{71}$$

with $x_1 = \dfrac{\rho(1+1/\mu)}{\beta(L+1)}$, $z_1 = \beta(L+1)$, $x_2 = \dfrac{\rho(1/\mu)}{\beta L}$, and $z_2 = \beta L$.

If $\beta > \dfrac{1}{L}$, then $z_1 > 1$, and $z_2 > 1$. By (65) we have

$$\lim_{\rho\to\infty} R_1(\rho,\mu,\beta) = 0 . \tag{72}$$

By (66) we have

$$\lim_{x\to\infty} R_2(\rho,\mu,\beta) = \beta(L+1)\log\frac{1}{1 - 1\big/\beta(L+1)} - \beta L \log\frac{1}{1 - 1\big/\beta L} . \tag{73}$$

$\lim_{\rho\to\infty} R_3(\rho,\mu,\beta)$ is in the form of $\log\dfrac{\infty}{\infty}$. By L'Hopital's rule, we have

$$\begin{aligned}\lim_{\rho\to\infty} \frac{1 + x_1 z_1 - \tfrac{1}{4}F(x_1,z_1)}{1 + x_2 z_2 - \tfrac{1}{4}F(x_2,z_2)} &= \lim_{\rho\to\infty} \frac{\dfrac{\partial}{\partial\rho}(1 + x_1 z_1 - \tfrac{1}{4}F(x_1,z_1))}{\dfrac{\partial}{\partial\rho}(1 + x_2 z_2 - \tfrac{1}{4}F(x_2,z_2))} \\ &= \frac{\dfrac{(1+1/\mu)}{z_1}(z_1 - 1)}{\dfrac{1/\mu}{z_2}(z_2 - 1)},\end{aligned} \tag{74}$$

where we use the fact that

$$\lim_{x_1\to\infty} \frac{\partial}{\partial x_1}(1 + x_1 z_1 - \tfrac{1}{4}F(x_1,z_1)) = z_1 - 1 \tag{75}$$

when $z_1 > 1$. Equation (54) follows after simple calculation.

If $\beta \le \frac{1}{L+1}$, then $z_1 \le 1$, and $z_2 < 1$. We have

$$\lim_{\rho\to\infty} R_2(\rho,\mu,\beta) = (z_1 - z_2)\log(1 + x_1 - \tfrac{1}{4}F(x_1,z_1)) + z_2 \log\left(\frac{1 + x_1 - \frac{1}{4}F(x_1,z_1)}{1 + x_2 - \frac{1}{4}F(x_2,z_2)}\right). \quad (76)$$

Similarly,

$$\begin{aligned}\lim_{\rho\to\infty} \frac{1 + x_1 - \frac{1}{4}F(x_1,z_1)}{1 + x_2 - \frac{1}{4}F(x_2,z_2)} &= \lim_{\rho\to\infty} \frac{\frac{\partial}{\partial\rho}(1 + x_1 - \frac{1}{4}F(x_1,z_1))}{\frac{\partial}{\partial\rho}(1 + x_2 - \frac{1}{4}F(x_2,z_2))} \\ &= \frac{\frac{(1+1/\mu)}{z_1}(1-z_1)}{\frac{1/\mu}{z_2}(1-z_2)},\end{aligned} \quad (77)$$

where we use the fact that

$$\lim_{x_1\to\infty} \frac{\partial}{\partial x_1}(1 + x_1 - \tfrac{1}{4}F(x_1,z_1)) = 1 - z_1 \quad (78)$$

when $z_1 \le 1$. As $z_1 > z_2$, by (66) we have

$$\lim_{\rho\to\infty} R_2(\rho,\mu,\beta) = \infty, \quad (79)$$

and (55) follows.

References

[1] E. Biglieri, J. Proakis, and S. Shamai, "Fading channels: information-theoretic and communications aspect," *IEEE Trans. Inform. Theory*, vol. 44, no. 6, pp. 2619-2692, Oct. 1998.

[2] D.W. Bliss, K.W. Forsythe, and A.F Yegulalp, "MIMO communication capacity using infinite dimension random matrix eigenvalue distributions," *Proc. 35th Asilomar Conf. Signals, Systems, Computers*, vol.2, pp. 969-974, Pacific Grove, CA, Nov. 2001.

[3] R. S. Blum, J. H. Winters and N. R. Sollenberger, "On the capacity of cellular systems with MIMO", *IEEE Communications Letters*, pp. 242-244, June 2002.

[4] R. S. Blum, "MIMO Capacity with Interference", *IEEE Journal on Selected Area in Communications*, Special issue on MIMO, to appear.

[5] A. R. Calderbank, "The art of signaling: Fifty years of coding theory," *IEEE Trans. Inform. Theory*, vol. 44, no. 6, pp. 2561-2595, Oct. 1998.

[6] S. Catreux, P. F. Driessen and L. J. Greenstein, "Simulation results for an interference-limited multiple-input multiple-output cellular system," *IEEE Commun. Lett.*, vol. 4, no. 11, pp. 334-336, Nov. 2000

[7] T. M. Cover and J. A. Thomas, *Elements of Information Theory*, New York: Wiley, 1991

[8] H. Dai, A. F. Molisch, and H. V. Poor: "Downlink capacity of interference-limited MIMO systems with joint detection," to appear in *IEEE Trans. Wireless Commun.*

[9] H. Dai, A. F. Molisch, and H. V. Poor: "Downlink multiuser capacity of interference-limited MIMO systems," *Proc. 2002 IEEE 13th International Symposium on Personal, Indoor and Mobile Radio Communications* (PIMRC), Lisbon, Portugal, Sept. 2002.

[10] H. Dai and A. F. Molisch: "Multiuser detection for interference-limited MIMO systems," *Proc. 2002 Spring IEEE Vehicular Technology Conf* (VTC)., CDROM, Birmingham, AL, May 2002.

[11] S. N. Diggavi, "On achievable performance of spatial diversity fading channels," *IEEE Trans. Inform. Theory*, vol. 47, no. 1, pp.308-325, Jan. 2001.

[12] G. D. Forney and G. Ungerboeck, "Modulation and coding for linear Gaussian channels," *IEEE Trans. Inform. Theory*, vol. 44, no. 6, pp. 2384-2415, Oct. 1998.

[13] G. J. Foschini and M. J. Gans, "On limits of wireless communications in a fading environment when using multiple antennas, " *Wireless Personal Communications*, vol. 6, no. 3, pp. 311-335, Mar. 1998.

[14] G. J. Foschini, G. D. Golden, R. A. Valenzuela and P. W. Wolniansky, "Simplified processing for high spectral efficiency wireless communication employing multi-element arrays," *IEEE J. Selected Areas Commun.*, vol. 17, no. 11, pp. 1841-1852, Nov. 1999.

[15] A. J. Grant and P. D. Alexander, "Random sequence multisets for synchronous code-division multiple-access channels," *IEEE Trans. Inform. Theory*, vol. 44, no. 7, pp.2832-2836, Nov. 1998.

[16] D. Jonsson, "Some limit theorems for the eigenvalues of a sample covariance matrix," *J. Multivariate Anal.*, vol. 12, pp. 1-38, 1982

[17] A. Lapidoth, "Mismatched decoding and the multiple-access channel," *IEEE Trans. Inform. Theory*, vol. 42, no. 6, pp. 1439-1452, Sept. 1996.

[18] A. Lapidoth, "Nearest neighbor decoding for additive non-Gaussian channels," *IEEE Trans. Inform. Theory*, vol. 42, no. 6, pp. 1520-1529, Sept. 1996.

[19] T. L. Marzetta and B. M. Hochwald, "Capacity of a mobile multiple-antenna communication link in Rayleigh flat fading," *IEEE Trans. Inform. Theory*, vol. 45, no. 1, pp. 139-157, Jan. 1999.

[20] H. V. Poor and S. Verdú, "Probability of error in MMSE multiuser detection," *IEEE Trans. Inform. Theory*, vol. 43, no. 3, pp. 858-871, May 1997.

[21] H. V. Poor, “Iterative multiuser detection,” *IEEE Signal Processing Magazine*, vol. 20, no. 6, Nov. 2003.

[22] P. B. Rapajic and D. Popescu, “Information capacity of a random signature multiple-input multiple output channel,” *IEEE Trans. Commun.*, vol. 48, no. 8, pp.1245-1248, Aug. 2000.

[23] S. Shamai (Shitz) and S. Verdú, “The impact of frequency-flat fading on the spectral efficiency of CDMA,” *IEEE Trans. Inform. Theory*, vol. 47, no. 3, pp.1302-1327, May 2001.

[24] S. Shamai (Shitz) and A. D. Wyner, “Information theoretic considerations for symmetric, cellular, multiple-access fading channels – parts I & II,” *IEEE Trans. Inform. Theory*, vol. 43, no. 6, pp.1877-1911, Nov. 1997.

[25] J. W. Silverstein and Z. D. Bai, “On the empirical distribution of eigenvalues of a class of large dimensional random matrices,” *J. Multivariate Anal*., vol. 54, no. 2, pp. 175-192, 1995

[26] J. W. Silverstein “Strong convergence of the empirical distribution of eigenvalues of large dimensional random matrices,” *J. Multivariate Anal*., vol. 55, pp. 331-339, 1995

[27] E. Telatar, "Capacity of multi-antenna Gaussian channels," *European Trans. Telecomm*., vol. 10, no. 6, pp. 585-595, Nov.-Dec. 1999.

[28] D. Tse and S. Hanly, “Linear multiuser receivers: effective interference, effective bandwidth and user capacity,” *IEEE Trans. Inform. Theory*, vol. 45, no. 2, pp.641-657, Mar. 1999.

[29] M. K. Varanasi and T. Guess, “Optimum decision feedback multiuser equalization with successive decoding achieves the total capacity of the Gaussian multiple-access channel,” *Proc. 31st Asilomar Conf. Signals, Systems, Computers*, vol.2, pp. 1405-1409, Pacific Grove, CA, Nov. 1997.

[30] S. Verdú, “Capacity region of Gaussian CDMA channels: the symbol-synchronous case,” *Proc. 24th Allerton Conf. Commun., Contr. and Comput.*, pp. 1025-1034, Allerton, IL, Oct. 1986.

[31] S. Verdú, *Multiuser Detection*, Cambridge, U.K.: Cambridge Univ. Press, 1998.

[32] S. Verdú and S. Shamai (Shitz), “Spectral efficiency of CDMA with random spreading,” *IEEE Trans. Inform. Theory*, vol. 45, no. 2, pp.622-640, Mar. 1999.

[33] A. D. Wyner, "Shannon-theoretic approach to a Gaussian cellular multiple-access channel," *IEEE Trans. Inform. Theory*, vol. 40, no. 6, pp.1713-1727, Nov. 1994.

[34] S. Ye and R. S. Blum, “Optimum signaling of MIMO-OFDM systems with interference”, *European Signal Processing Conference*, Toulouse, France, 2002.

[35] B. M. Zaidel, S. Shamai (Shitz) and S. Verdú, “Multicell uplink spectral efficiency of coded DS-CDMA with random signatures,” *IEEE J. Selected Areas Comm.*, vol. 19, no.8, pp. 1556-1569, Aug. 2001.

[36] J. Zhang, E. K. P. Chong and D. Tse, “Output MAI distributions of linear MMSE multiuser receivers in CDMA systems,” *IEEE Trans. Inform. Theory*, vol. 47, no. 3, pp.1128-1144, May 2001.

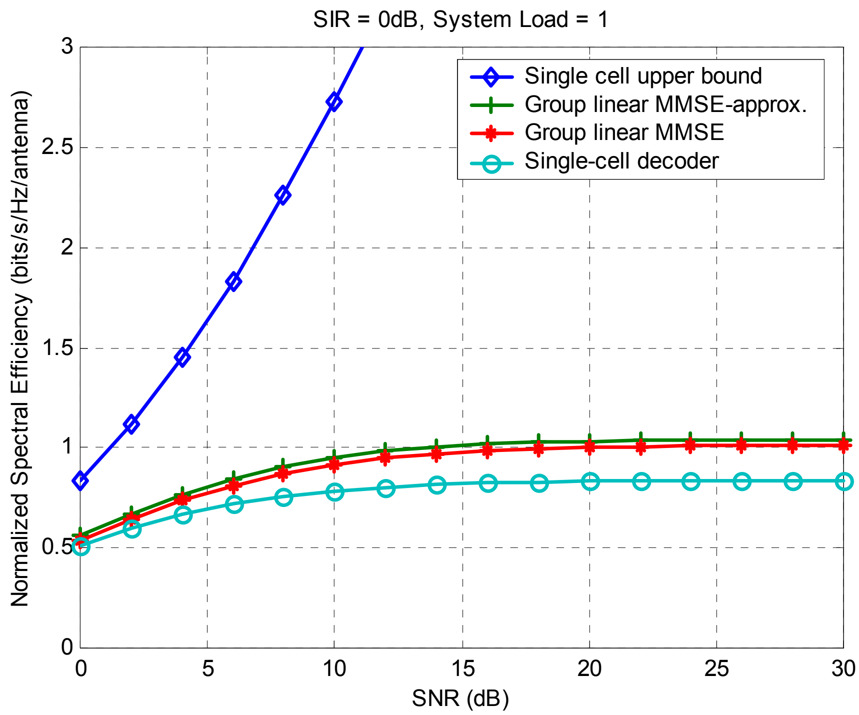
SIR = 0dB, System Load = 1
Single cell upper bound
Group linear MMSE-approx.
Group linear MMSE
Single-cell decoder
Normalized Spectral Efficiency (bits/s/Hz/antenna)
SNR (dB)
0
0.5
1
1.5
2
2.5
3
0
5
10
15
20
25
30

(a)

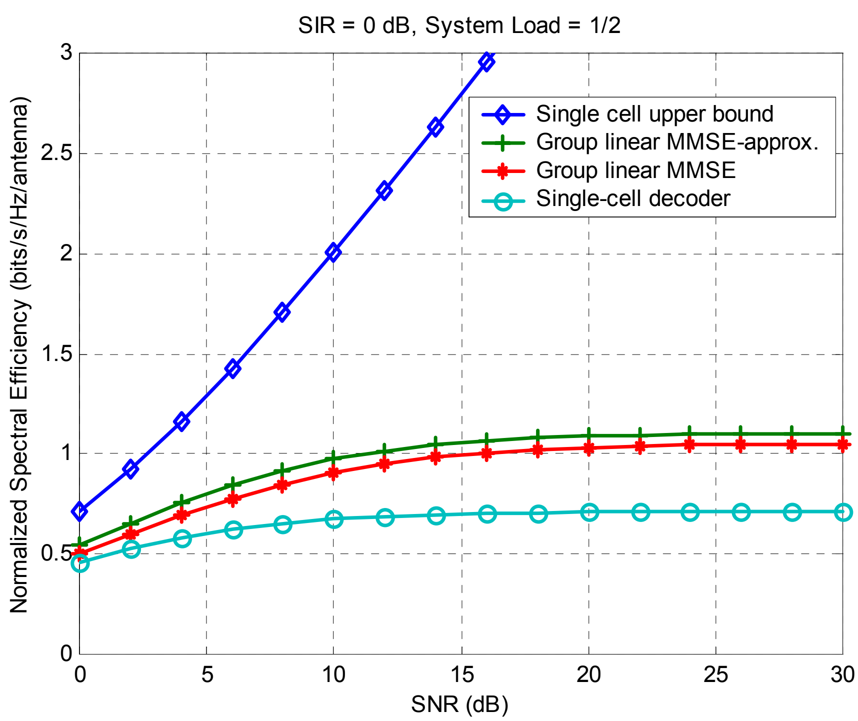
SIR = 0 dB, System Load = 1/2
Single cell upper bound
Group linear MMSE-approx.
Group linear MMSE
Single-cell decoder
Normalized Spectral Efficiency (bits/s/Hz/antenna)
SNR (dB)
0
0.5
1
1.5
2
2.5
3
0
5
10
15
20
25
30

(b)

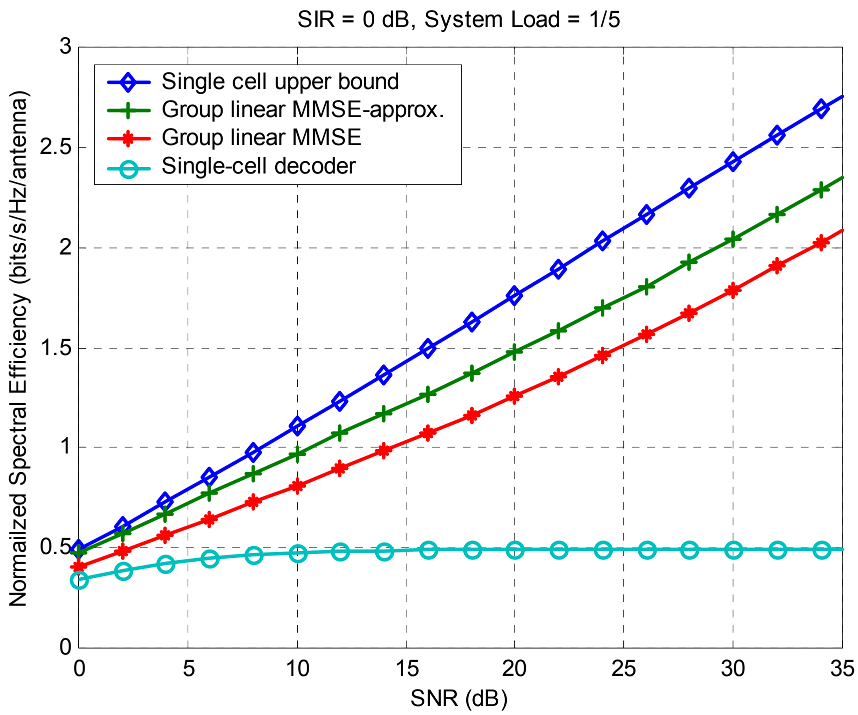

(c)

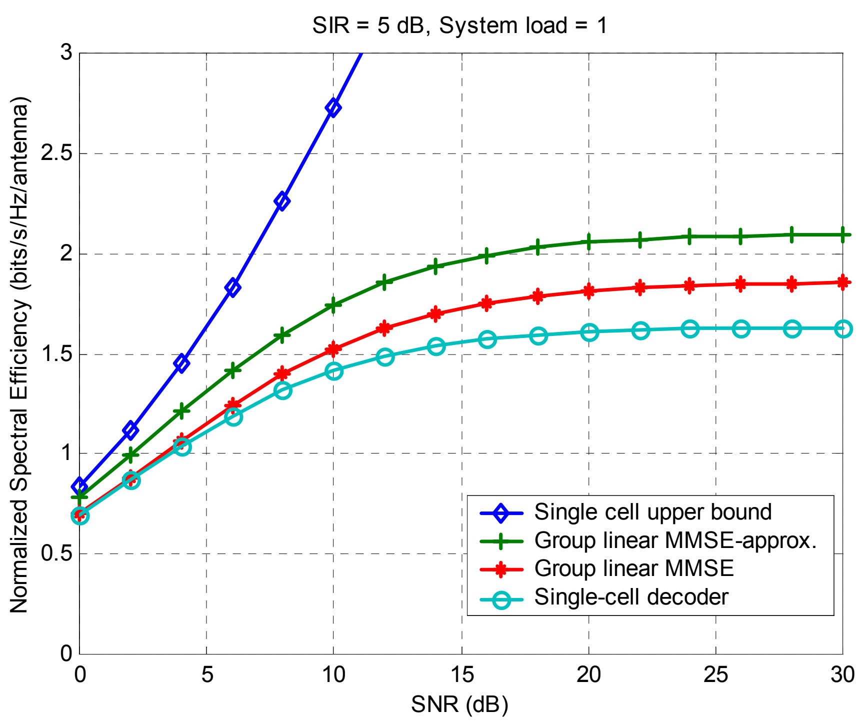

(d)

Fig. 1 Study of the interference-limited behavior of various multicell MIMO spectral efficiencies

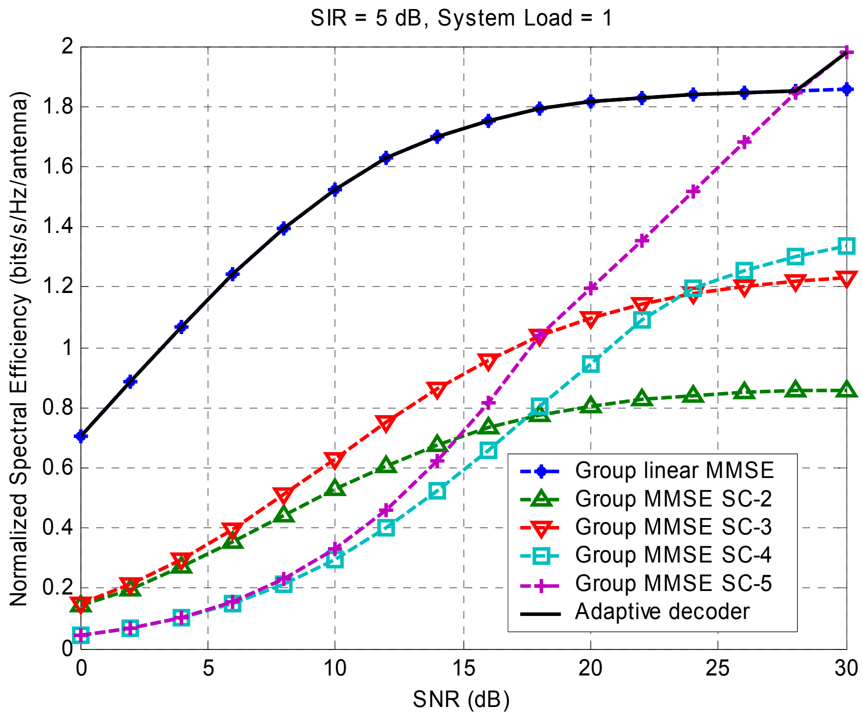
SIR = 5 dB, System Load = 1
Normalized Spectral Efficiency (bits/s/Hz/antenna)
SNR (dB)
Group linear MMSE
Group MMSE SC-2
Group MMSE SC-3
Group MMSE SC-4
Group MMSE SC-5
Adaptive decoder

(a)

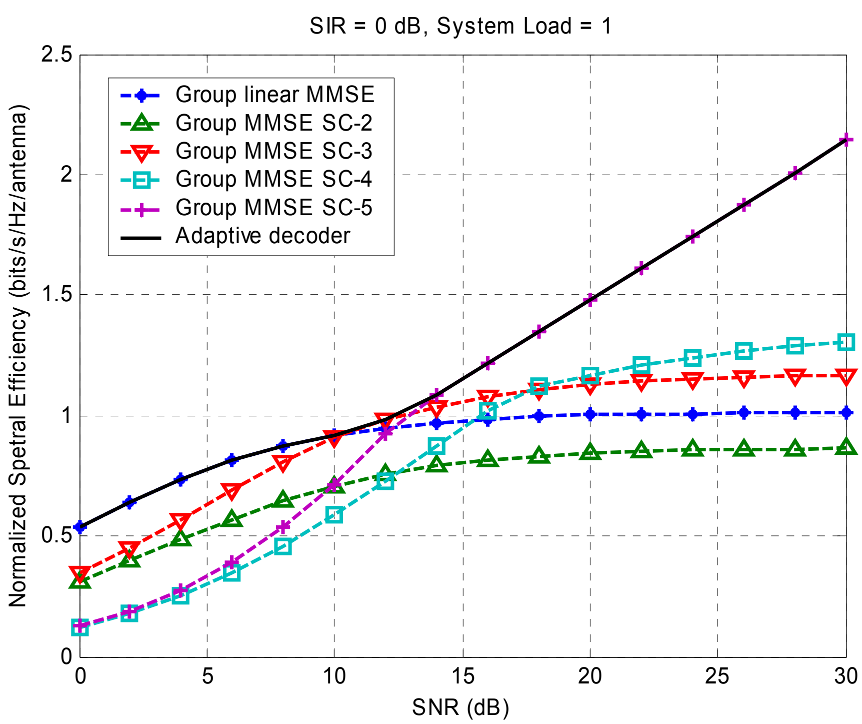
SIR = 0 dB, System Load = 1
Normalized Spetral Efficiency (bits/s/Hz/antenna)
SNR (dB)
Group linear MMSE
Group MMSE SC-2
Group MMSE SC-3
Group MMSE SC-4
Group MMSE SC-5
Adaptive decoder

(b)

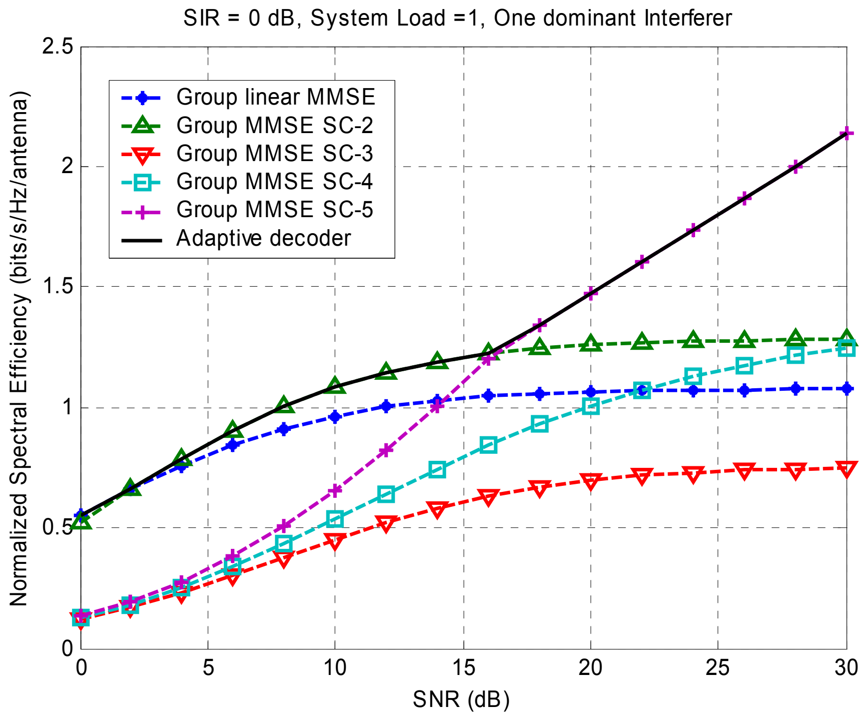

(c)

Fig. 2 Spectral efficiency comparison of the group linear MMSE detector, the group MMSE successive interference cancellation detector, and the adaptive detector

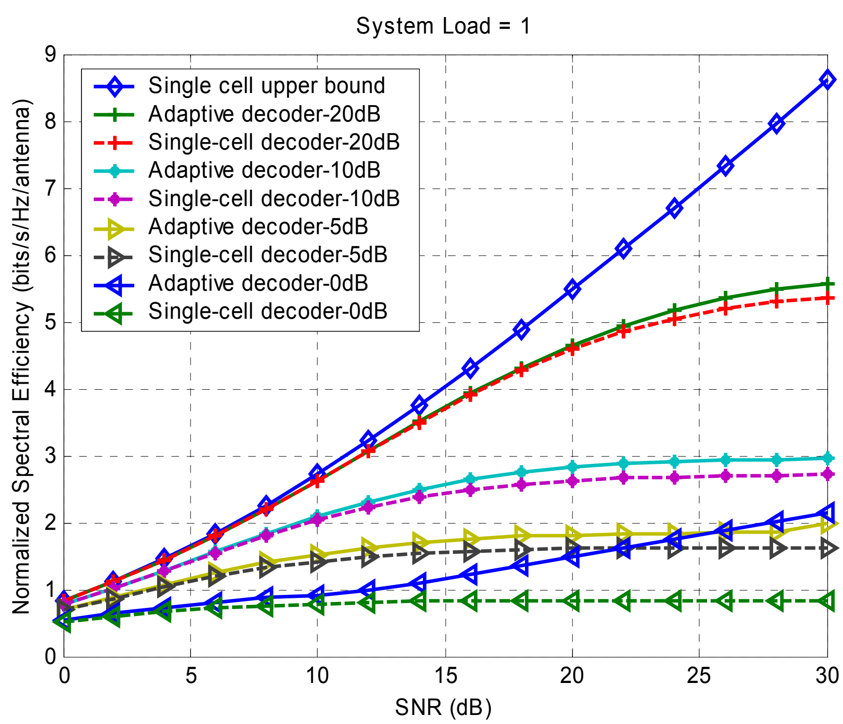

(a)

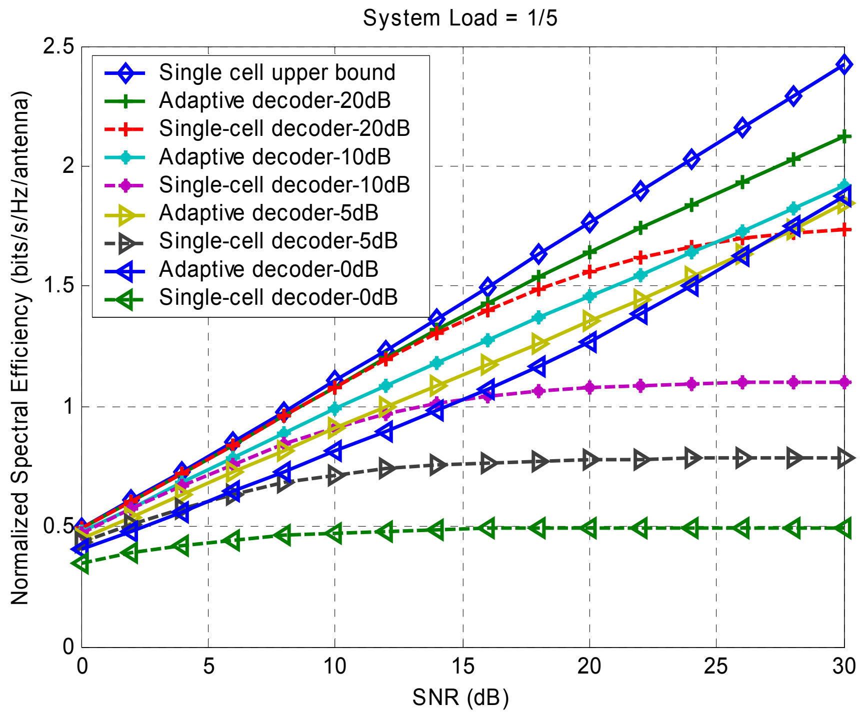

(b)

Fig. 3 Multicell MIMO spectral efficiencies for different SNRs and SIRs